Real-time spatial concentration measurement under versatile temperature and concentration conditions using a conventional interferometry

D. C. Yin[a,b], Y. Inatomi[c,*], N. I. Wakayama[b], W. D. Huang[a]

[a]*State Key Lab Solidification Processing, Northwestern Polytechnical University, Xi'an 710072, Shaanxi, PR China*

[b]*National Institute of Advanced Industrial Science and Technology, 1-1-1 Higashi, Tsukuba, Ibaraki 305-8565, Japan*

[c]*Space Utilization Research Center, The Institute of Space and Astronautical Science, 3-1-1Yoshinodai, Sagamihara, Kanagawa 229-8510, Japan*

[*]Corresponding author. Space Utilization Research Center, The Institute of Space and Astronautical Science, 3-1-1Yoshinodai, Sagamihara, Kanagawa 229-8510, Japan. Tel.: +81-42-759-8529; fax: +81-42-759-8530. e-mail: inatomi@surc2.isas.ac.jp

Abstract: This paper describes a simple protein concentration measurement system using Mach-Zehnder interferometry that allows monitoring of the time course evolution of the protein concentration distribution (concentration map) during the protein crystal growth or dissolution processes under versatile temperature and concentration conditions. A measurement program package has been developed to achieve probing of the concentration map. The measurement is based on the relationship between the refractive index and the concentration of the solution. The phase shift of the interferogram gives the information of the variation of the refractive index, which can be converted to the change of the concentration, making it easy to obtain the absolute level of the solute concentration in the solution. After the elimination of errors (or noises) caused by the environmental reasons by taking the bottom of the sample cell as reference, this non-invasive technique was proved to be a highly reliable and powerful tool to monitor the concentration variation in the solution. The stability of the protein crystal growth processes under isothermal and gradient temperature conditions were studied using this system. It was found that the crystal growth process under a temperature gradient control is much more stable than the case in isothermal condition. The statistical error of the lysozyme concentration under vertical temperature gradient control is less than ±0.43 $mg \cdot ml^{-1}$; while in the

isothermal condition, the concentration evolution shows large discrepancies (sometimes more than 10 $mg \cdot ml^{-1}$ in the concentration) between the different experimental runs despite that the experimental conditions were controlled to be the same. This technique may be applied to other solution systems where real-time monitoring of solute concentration map is necessary under diverse temperature and concentration conditions.

Keywords: A1. Biocrystallization; A1. Concentration measurement; A2. Growth from solutions; B1. Biological macromolecules; B1. Lysozyme; B3. Interferometry;

PACS: 06.30.-k; 07.05.Hd; 07.60.Ly; 81.10.Dn

1. Introduction

Concentration evolution of solute during solution crystal growth provides important mass transport information which facilitates understanding of the growth process of the crystals. The measurement of the solute concentration thus becomes essential for the scientists who are interested in the mechanisms or the processes of the crystal growth. Protein concentration measurement techniques have been extensively exploited since the last century. Numerous measurement techniques have been developed. Now we know that the concentration of a specific protein in a solution may be determined through many ways, some of which are now widely available commercially, such as UV absorption spectrophotometry (for example, absorbance 280 nm assay) [1-3], the biuret assay [4-6], Lowry assay [7], protein binding dyes method [8], bicinchoninic acid (BCA) method [9], *o*-phthalaldehyde (OPA) fluorescent protein assay [10], magnetic resonance [11], *etc*., and some other non-invasive techniques developed for monitoring the protein concentration during the crystal growth process, like Raman spectroscopy [12], near infrared spectroscopy [13], and interferometry [14-23]. Among the above techniques, interferometry is a quite promising method in that it can provide information of the spatial concentration distribution of the solute, temperature profile, shape contour map, and even convection in a fluid [24]. As such a powerful tool the interferometry technique has been widely applied in the crystal growth studies, mainly in monitoring advancement of the solid face [25-28], and determination of the concentration field [14-23].

In the field of concentration measurement using the interferometry, generally the techniques can be divided into two groups: conventional interferometry and phase-shift interferometry. The latter was developed in 1970s [29], and soon found applications in many fields for its high resolution capability. It has been also applied in the field of solution concentration measurement [14, 17, 22]. In crystal growth or dissolution systems, as the concentration is varying with time, it is very important to capture all the modulated interferograms simultaneously to ensure that the calculated phase is the right one at the capture time. Generally the efforts to avoid the acquisition of different interferograms at different times can be made by generating the phase-shifted interferograms at spatially different positions [30], so that the capturing of different phase-shifted patterns can be carried out synchronously. By using polarizers arranged at different orientations, Onuma *et al.* [14] succeeded in getting three interferograms simultaneously, enabling the system to analyze the concentration of $NaClO_3$ around the crystal in real time. Such techniques are promising in monitoring systems if the errors caused by the utilization of different optical parts can be minimized, but they may not be suitable in some special cases due to the limitations of the experimental setups, for example, due to the compact size of the setup, or any extreme conditions like a strong magnetic field in which the polarization of light will be rotated because of the Faraday effect. Compared with the phase-shift interferometry techniques, the conventional interferometry is still very useful in that it can easily achieve real time monitoring of the varying target parameters without taking any measures to succeed the simultaneity for the captures because it needs only one interferogram at one time. If its measurement accuracy meets the requirement of the study, the conventional technique will be still useful and competitive for its simplicity and low cost.

To date there is no report of the time evolution monitoring of the spatial concentration distribution of protein in the solution during crystal growth or dissolution processes using the conventional interferometry. Furthermore, in the previous literatures most reports on the concentration measurement using interferometry were related to isothermal conditions. In this paper the authors developed a lysozyme concentration measurement system which can be used in varying temperature and concentration conditions. A measurement program was developed to carry out the concentration calculation, enabling monitoring of the concentration profile in the observation field in real time. The concentration effect of NaCl, as one important component in the solution, on the measurement result

was discussed. Finally, the stabilities of the lysozyme crystal growth under different temperature conditions were also studied using this system.

2. Measurement principle

The optical properties of a solution, like refractive index, are functions of the solute concentration and temperature. Through the relationship between the concentration and the refractive index, the concentration of the solute in the solution can be obtained by determining the refractive index of the solution. Monitoring of the concentration can be therefore achieved by monitoring of the refractive index. Interferometry can make possible to monitor the refractive index simply and sensitively.

Let's consider a sample cell with solution as illustrated in Fig. 1. The laser beam direction is normal to the sidewall of the cell. We assume that along this light direction the concentration is homogeneous (in more practical cases when the concentration is not homogeneous especially when the solution thickness is large, the concentration here represents its average level over the thickness of the solution in the direction of the light), so that we can treat the problem two dimensionally. Every point in the observed region can be expressed by an orthogonal coordinate (x,y). (See Fig. 1., the schematic illustration of the cell).

If we study the solution only, and suppose that the initial refractive index of the solution is $n_0(x,y)$; after a short period of time Dt, the refractive index changes to $n(x,y)$ at point (x,y) for some reasons (like temperature change and/or concentration change). If the phase change at point (x,y) is $Df(x,y)$, then we have:

$$[n(x,y)-n_0(x,y)]d=\frac{l}{2p}\Delta f(x,y), \tag{1}$$

where l: the wavelength of the light beam, d: the thickness of the solution in the direction of the optical pathway.

At a certain wavelength, the refractive index is a function of the temperature and the solute concentration [31]:

$$\Delta n(x,y)=n(x,y)-n_0(x,y)=\left[\frac{\partial n_s}{\partial C}\right]_T\Delta C(x,y)+\left[\frac{\partial n_s}{\partial T}\right]_C\Delta T(x,y), \tag{2}$$

where $Dn(x,y)$, $DC(x,y)$ and $DT(x,y)$ are the refractive index, the concentration and temperature differences at the point (x,y), respectively.

Thus we have

$$\left\{\left[\frac{\partial n_s}{\partial C}\right]_T [C(x,y)-C_0(x,y)]+\left[\frac{\partial n_s}{\partial T}\right]_C [T(x,y)-T_0(x,y)]\right\}d=\frac{l}{2p}\Delta f(x,y), \quad (3)$$

where $C_0(x,y)$: the initial concentration at (x,y), $T_0(x,y)$: the initial temperature at (x,y), $T(x,y)$: the temperature at (x,y), and $C(x,y)$: the concentration at (x,y).

From Eq. (3), we obtain:

$$C(x,y)=C_0(x,y)+\left\{\frac{l}{2pd}\Delta f(x,y)-\left[\frac{\partial n_s}{\partial T}\right]_C [T(x,y)-T_0(x,y)]\right\}/\left[\frac{\partial n_s}{\partial C}\right]_T . \quad (4)$$

This is the basic equation for the calculation of the concentration using interferometry under versatile temperature and concentration conditions. At a given temperature program, the concentration of the solute can be obtained at any point (x,y) in the observation field through monitoring the phase change $Df(x,y)$.

3. Determination of optical parameters necessary for measurement

It is important to measure some optical parameters before the concentration measurement because they are indispensable for the concentration calculation. If the solution is kept under a constant temperature, at least the dependence of the refractive index of the solution on the concentration ($[\partial n_s/\partial C]_T$) should be known. If the temperature changes during the process, other two parameters are necessary: the dependence of the refractive index of protein solution on temperature ($[\partial n_s/\partial T]_C$), and the dependence of the refractive index of the container on temperature ($[\partial n_q/\partial T]$).

Fredericks *et al.* gave a comprehensive report about the physical properties of lysozyme solution [32], the dependences of refractive index of the solution (at the sodium D-line, 589 nm) on temperature and on concentration were included. Other researchers [20, 21, 33, 34] also reported their own results under different conditions. However, if we hope to study the concentration change during the process while the temperature is varying with time, the data provided in the literatures (mostly suitable for isothermal process) are not enough for the purpose. Furthermore, the actual experimental conditions might be different if the light source with different wavelengths, or different solution conditions are used. Therefore it is necessary to calibrate specifically before starting actual concentration measurement.

In this work, we used the measurement system described currently to determine the parameters at wavelength λ= 780nm. Detailed measurement techniques will be presented elsewhere. The calibrated results are listed below:

(1) Temperature dependence of refractive index of cell quartz [$\P n_q/\P T$]:

[$\P n_q/\P T$] =(8.49±0.05)×$10^{-6}K^{-1}$. ().

(2) Concentration dependence of refractive index of the lysozyme solution:

[$\partial n_s/\partial C]_T \approx$Constants= (2.16 ± 0.**41**)×10^{-4}ml·mg^{-1}.

(3) Temperature dependence of refractive index of the lysozyme solution (in the temperature range 0~60°C):

(4) The following empirical equation was obtained to predict [$\partial n_s/\partial T]_C$ at different concentrations:

$$\left[\frac{\partial n_s}{\partial T}\right]_C = 2.477\times10^{-9}C^2 - 3.511\times10^{-7}C - 1.411\times10^{-4}, \quad (5)$$

where C is the concentration. The results of [$\partial n_s/\partial T]_C$ at the concentration 0 ~ 70 mg·ml^{-1} were found to be in the range of -1.41×$10^{-4}K^{-1}$~-1.54×$10^{-4}K^{-1}$.

The above measurement data enable the determination of lysozyme concentration not only at homogeneously constant temperature conditions, but also at various conditions when the temperature varies in the process, or even varies differently at different positions at the same time, thus making the concentration measurement method using interferometry more versatile and powerful. These parameters will also be applicable for other purpose where the temperature or concentration dependence of the refractive index of lysozyme solution is necessary.

4. Effect of NaCl concentration on concentration measurement result

Protein crystal growth system is complicated since it involves four or more components (protein molecule, water, precipitant and counterion) during the crystallization process. Precipitant is indispensable in the system to adjust the interactions between the protein molecules so that crystallization can occur. In our case we used NaCl as precipitant. Strictly speaking, precipitant NaCl in the solution will contribute to the phase change if the concentration of NaCl changes during the measurement. Generally the effect of NaCl on the measurement result is neglected because the change of the concentration in the solution is very small compared with HEWL [35]. However, for accurate measurement we should check the effect of NaCl on the result because NaCl concentration is subject to change in the solution during the crystal growth when NaCl incorporates into the crystal.

If we consider the solution only, during the measurement the phase shift should consist of two parts caused by the concentration variations of NaCl and lysozyme, respectively:

$$\frac{\Delta f}{2p} l = (\Delta n_{lys} + \Delta n_{NaCl})d = \{[(\frac{\partial n}{\partial T})_C \Delta T + (\frac{\partial n}{\partial C})_T \Delta C]_{lys} + [(\frac{\partial n}{\partial T})_C \Delta T + (\frac{\partial n}{\partial C})_T \Delta C]_{NaCl}\}d \quad , \tag{6}$$

where, for simplicity, the position coordinate (x,y) is removed from the following equations and the subscripts "*lys*" and "*NaCl*" represent that of solute lysozyme and precipitant NaCl, respectively.

In the actual concentration measurement in our method (also in most other scientists' methods), we take the relationship like this:

$$\frac{\Delta f}{2p} l = \Delta n_{lys} d = [(\frac{\partial n_s}{\partial T})_C \Delta T + (\frac{\partial n_s}{\partial C})_T \Delta C]d \ . \tag{7}$$

Here both $[\partial n_s/\partial C]_T$ and $[\partial n_s/\partial T]_C$ are treated as that of lysozyme, but actually they are combined products of the refractive index changes caused by lysozyme and NaCl in pure water.

It's necessary to check the relationship between the actual measured and the true concentration levels in order to reveal the influence of this treatment is to the final calculation.

During the calibration measurement of the physical parameters,

$$(\frac{\partial n}{\partial C})_{T-cal} \Delta C_{Lys-cal} = (\frac{\partial n}{\partial C})_{T-Lys-true} \Delta C_{Lys-cal} + (\frac{\partial n}{\partial C})_{T-NaCl-true} \Delta C_{NaCl-cal} \ , \tag{8}$$

where the subscripts "*cal*" and "*true*" represent that of the parameters obtained or used in the calibration, and that of the true values of the parameters, respectively. $(\frac{\partial n}{\partial C})_{T-cal}$ is the parameter we used for the subsequent concentration measurement:

$$(\frac{\partial n}{\partial C})_{T-cal} = (\frac{\partial n}{\partial C})_{T-Lys-true} + (\frac{\partial n}{\partial C})_{T-NaCl-true} \frac{\Delta C_{NaCl-cal}}{\Delta C_{Lys-cal}} \ . \tag{9}$$

In an actual measurement process without temperature change:

$$(\frac{\partial n}{\partial C})_{T-cal} \Delta C_{Lys-meas} = \Delta n = (\frac{\partial n}{\partial C})_{T-Lys-true} \Delta C_{Lys-true} + (\frac{\partial n}{\partial C})_{T-NaCl-true} \Delta C_{NaCl-true} \ , \tag{10}$$

where the subscript "*meas*" represents that of the measured result.

Thus:

$$(\frac{\partial n}{\partial C})_{T-cal} = (\frac{\partial n}{\partial C})_{T-Lys-true}(\frac{\Delta C_{lys-true}}{\Delta C_{Lys-meas}}) + (\frac{\partial n}{\partial C})_{T-NaCl-true}(\frac{\Delta C_{NaCl-true}}{\Delta C_{Lys-meas}}). \quad (11)$$

Apparently, comparing Eq. (11) with Eq. (9), we can see $\Delta C_{Lys-meas} = \Delta C_{Lys-true}$ if we assume:

$$(\frac{\Delta C_{NaCl}}{\Delta C_{Lys}}) = \text{constant} \quad (12)$$

Support for this assumption can be found in the previous experiments [36] that the salt is strongly coupled with lysozyme molecules.

$$\frac{\Delta C_{NaCl-true}}{\Delta C_{Lys-true}} = \frac{\Delta C_{NaCl-cal}}{\Delta C_{Lys-cal}}, \quad (13)$$

then.

For the case when the temperature changes, by using the same method, we can obtain:

$$(\frac{\partial n}{\partial T})_{C-lys-cal} = (\frac{\partial n}{\partial T})_{C-lys-true} + (\frac{\partial n}{\partial T})_{C-NaCl-true}. \quad (14)$$

As the temperature change is always supposed to be the same for both NaCl and lysozyme, we can use the above-calibrated data to substitute the true values without causing any error in the measurement.

In conclusion, we take the calibrated data of the physical parameters to calculate the concentration, the final result should be reliable.

5. Measurement system

Fig. 2. gives an illustration of the current measurement system. Fig. 2. (a) shows the optical system and the concentration measurement system. The optical system is a Mach-Zehnder interferometer. LD (Laser diode) is the light source with wavelength 780 nm. The interferometer mainly consists of two beam splitters BS1 and BS2, and two mirrors M1 and M2. The sample cell is put to the pathway of one separated beam; another one is taken as the reference beam. CP is a compensator, which is used to compensate the optical path difference caused by the insertion of the sample cell to the optical pathway. W is the wedge for the adjustment of the fringe images. The sample cell is fixed to the interferometer using a sample holder, which is a combination of a pair of Peltier devices and a water-cooling system (Fig. 2. (b)). Temperatures of the upper and lower part of the sample cell could be controlled by the Peltier devices with a high temperature control accuracy up to ±0.1°C separately in the range of 0~60℃. The interferograms are captured by a CCD camera with 640×480 pixels and sent to a computer for

intensity analysis, concentration calculation, and display of the interference images. These images are also sent to a videocassette recorder (VCR) to preserve the processes for further possible reference. Another computer is connected to the main computer to display the results of the time dependence of the concentration evolution. Fig. 3 gives a block diagram of the measurement programs including a main program to calculate the concentration and a display program to show the result.

6. Measurement example

Here we will give an example of the concentration measurement during the dissolution process of the lysozyme tetragonal crystals to show the procedures.

6.1. Experiment procedures:

Hen egg white lysozyme (HEWL: from Seikagaku Kogyo, six times recrystallized) was used in this measurement. A layer of the HEWL crystals for the subsequent dissolution was prepared in advance. The initial conditions of the aqueous solution are as follows: HEWL: 45 $mg \cdot ml^{-1}$, NaCl: 40 $mg \cdot ml^{-1}$, and pH=4.60. No buffer was used. The inner dimensions of the cell are: height: 10mm, length: 15mm, and inner thickness of the container: 3mm. The crystal layer was prepared by keeping the cell under a temperature gradient, *i.e.*, 50°C at the upper end of the cell, 6°C at the lower end, for 21 hours. Then both temperatures of the upper and lower ends were changed to 25°C, and kept at such isothermal conditions for 3 hours.

The dissolution process of the crystals was started by increasing both temperatures at upper and lower sides. The temperature at the lower side was increased from 25°C to 50°C, and the upper temperature was increased from 25°C to 55°C simultaneously in 30min; then the temperature profile was kept until the end of the experiment. Fig. 4. schematically shows the temperature program.

6.2. Results and discussions

6.2.1. Concentration map acquisition

Fig. 5. (a) ~ (d) show the processes for obtaining the concentration map. First a fringe image was captured. Fig. 5. (a) shows such an image captured at 30 min from the start of the dissolution. The gray scale of the image can be taken as the light intensities of the interference, which can be used for phase analysis. The gray scale of every pixel in the image was obtained by scanning the image horizontally

from the left to the right. Fig. 5. (b) shows a figure of the interference intensities of one scanning line after one scan at 3mm above from the cell bottom. The phase of every studied point in the image can be calculated based on the light intensities analysis. As there was only one captured interferogram for each moment, the phase was calculated using the conventional way according to the positions of intensity maxima and minima. After the phase calculation, phase-unwrapping is necessary. The phase unwrapping in the current work is very easy because the fringe arrangement is simple and regular compared with those complicated fringe images (as in the three dimensional face contour measurement). According to the fact that the phase distribution from left to the right changes monotonously (increasing as arbitrarily determined in this system), the phase unwrapping can be done by comparing the phase difference between the adjacent points in a scanned line. If a jump occurred between the two adjacent points, the phase is unwrapped by adding or deducting 2π. Fig. 5. (c) shows a three dimensional view of the phase map (unwrapped) at 30min after the dissolution start. The final step is to resolve the phase map to concentration map. This can be succeeded using the principle stated in Section II. Fig. 5. (d) gives a three dimensional view of the concentration map at the same time.

6.2.2. Time course of concentration evolution

The time course of the concentration evolution at any point in the observation field can be extracted from the resulting measurement data and displayed in real-time in another computer. Fig. 6. (a) and (b) show the time evolutions of the phase and the concentrations at two selected points (3 mm and 2 mm above from the cell bottom at the center of the horizontal line) in the observation field, respectively. This is improved compared with our previous dissolution study [37] in which only the results of several selected points were obtained as we measured the concentration evolution manually.

6.2.3. Elimination of environmental errors

The errors (or noises) caused by the environmental reasons can be very large (sometimes more than $1mg \cdot ml^{-1}$) especially in the case of protein crystal growth and dissolution processes, because these processes take rather long time. In such a long time the unstable environmental conditions can be prominent to make the measurement results unreliable [16, 21].

Fortunately we can study the small region around the cell bottom, where the laser beam passes through both regions: (1) →quartz→solution→quartz (at the upper part of the observation region), and (2)

→quartz only (at the lower part of the observation region). At point (x,y) of the upper region, the total phase shift $Df(x,y) = Df_{q1}(x,y) + Df_s(x,y) + Df_{q2}(x,y) + Df_e(x,y)$, where $Df_{q1}(x,y)$ and $Df_{q2}(x,y)$ are the phase shifts caused by the temperature change of the quartz at both sides of the solution, respectively, $Df_s(x,y)$ is the phase shift caused by the solution changes (temperature and/or concentration), and $Df_e(x,y)$ is the phase shift caused by the environmental reasons. At point (x,y) of the lower part, the total phase shift is much simpler: $Df(x,y) = Df_q(x,y) + Df_e(x,y)$, where $Df_q(x,y)$ is the phase shift caused by the temperature change of the quartz. As the whole observation region is quite small (less than 4.8×6.4mm^2) so that we can take the environment induced phase shift as the same at both (x,y_{upper}) and (x,y_{lower}) points: $Df_e(x,y_{lower}) = Df_e(x,y_{upper})$. Therefore by taking the lower part of the cell as the reference we can easily eliminate the error caused by the environmental reasons.

6.2.4 Error analysis:

Statistical error: Statistical error is important for scientific research. Confident experimental measurements of any target parameters can be carried out only when the statistical error is small enough (for example, smaller than the difference between the comparing quantities). Statistical error may arise from any minute vibrations in the measurement apparatus, quantum uncertainties in the system, and many other small but uncontrollable factors. Smaller statistical error for the same experimental conditions represents better reproducibility of the experiment, thus the measurement system can be most valuable when the statistical error is small. Generally the crystal growth process of protein is not easy to control precisely. The growth sites and the concentration field may vary largely even if they are carried out in the same conditions.

Using the current measurement system we studied the stabilities of the lysozyme crystal growth under isothermal and temperature gradient controlled conditions starting from the as-prepared solution. The as prepared aqueous solution conditions are: HEWL: 51.7 mg·ml^{-1}, NaCl: 34.5 mg·ml^{-1}, pH=4.60.

Fig. 7. shows the results of several experimental runs. The dashed lines are the results obtained under a temperature gradient control (30°C at the upper end of the cell, and 10°C at the lower end of the cell), and the solid bold lines are the results obtained under isothermal condition (at 20°C). It is evident that the uncertainty of the crystal growth under isothermal conditions is much larger than that under temperature gradient controlled conditions. The reproducibility of the crystal growth process is very

poor in isothermal conditions, whereas in temperature gradient controlled conditions, the statistical error is small. The current results exhibit a statistical error of ±0.43 mg·ml^{-1} under the temperature gradient control. This is much better than those using isothermal condition in which the difference in the concentration can be as large as more than 10 mg·ml^{-1}. From these measurements we know that the temperature gradient control can largely improve the reproducibility of the protein crystal growth process. The reason for the better reproducibility of the concentration results under temperature gradient controlled conditions might come from the smaller difference in the growth area. When the nucleation and growth were controlled under the temperature gradient conditions, nearly all of the crystals were grown at the cell bottom. When the cell bottom was covered by the crystals, the growth of the crystals is restricted in the nearly the same limited area, thus if the growth rate is the same, the consumption of the solute will be (nearly) the same. While in the case of isothermal conditions, the crystals will nucleate everywhere in the cell, the total area of the growth faces will be strongly affected by the number of the nuclei and the positions of them. Larger area of the growth faces will no doubt increase the consumption of the solute in the solution. Thus for comparing experiments of protein crystal growth process the growth of seed crystals under temperature gradient control is recommended based on this experimental result.

Accuracy: the accuracy of the final result is determined by all the parameters used during the measurement. Generally in the conventional interferometry measurement we allow for 10% error in the phase shift determination. According to Onuma's work [14], phase-shift technique can achieve 25 times better resolution than conventional technique. Although (1) better resolution doesn't mean better accuracy, (2) the limitation of the resolution of the CCD camera will also make the resolution of both techniques to be nearer to each other, for convenience in the comparison, here we still assume that the phase measurement accuracy of the phase-shift technique can also achieve 25 times better accuracy, *i.e.*, the phase measurement error is less than 0.4%. The uncertainties of the other parameters for both the conventional and phase-shift techniques are assumed to be the same. For example, we use: λ: 780±10nm, d: 3000±50μm, $[\partial n_s/\partial T]_C$: -1.47×10^{-4}K^{-1}±1.3×10^{-5}K^{-1}, $[\partial n_s/\partial C]_T$: 2.14×10^{-4}±0.41×10^{-4} ml·mg^{-1} to estimate the error. If the system is controlled strictly without any temperature change, then the final measurement error will be ±0.26 mg·ml^{-1} for conventional system and ±0.23 mg·ml^{-1} for the phase-shift technique. That is to say, the difference of the final measurement accuracy is not so large as

that of the phase accuracy. The accuracy for both techniques may be highly improved if the errors come from the above-stated parameters can be reduced. In that case the phase-shift technique can achieve two or three times better accuracy over the conventional interferometry. But the accuracy difference between the two is still far smaller than the difference in their resolution capability. If the accuracy meets the minimum requirement of the study, the current studied technique should be very useful for its privileges in low cost and simplicity, and versatile application conditions.

7. Summary

In this paper a real-time protein concentration measurement system using a conventional Mach-Zehnder interferometer has been established. Such system can be used in a versatile temperature and concentration conditions to measure the spatial concentration distribution in the solution. Using this system, the reproducibility of lysozyme crystal growth under isothermal and temperature gradient controlled conditions are studied. It was found that temperature gradient conditions result in a much better reproducibility over the isothermal conditions.

Acknowledgement

This work was partially supported by the JSPS (Japanese Society for the Promotion of Science) Postdoctoral Fellowship Program, and EYTP (the Excellent Young Teachers Program of MOE，PR. China).

References:

[1] E. Layne, Methods in Enzymology 3 (1957) 447.

[2] C. M. Stoscheck, Methods in Enzymology 182 (1990) 50.

[3] G. L. Peterson, Methods in Enzymology 91 (1983) 95.

[4] E. M. Davis, Am. Biotech. Lab. 6 (1988) 28.

[5] C. V. Sapan, R. L. Lundblad, N. C. Price, Biotech. Appl. Biochem. 29 (1999) 99.

[6] A. G. Gornall, C. J. Bardawill, M. M. David, J. Biol. Chem. 177 (1949) 751.

[7] O. H. Lowry, N. J. Rosebrough, A. L. Farr, R. J. Randall, J. Biol. Chem. 193 (1951) 265.

[8] M. M. Bradford, Anal. Chem., 72 (1976) 248.

[9] P. K. Smith, R. I. Krohn, G. T. Hermansen, A. K. Malia, F. H. Gartner, M. D. Provenzano, E. K. Fujimoto, N. M. Goeke, B. J. Olson, D. C. Klenk, Anal. Chem., 150 (1985) 76.

[10] M. Roth, Anal. Chem. 43 (1971) 880.

[11] X. Q. Jiao, R. G. Bryant, Magnetic Resonance in Medicine 35 (1996) 159.

[12] A. M. Schwartz, K. A. Berglund, J. Crystal Growth 210 (2000) 753.

[13] J. T. Olesberg, M. A. Arnold, S. Y. B. Hu, Anal. Chem. 72 (2000) 4985. ----Search the database

[14] K. Onuma, K. Tsukumoto, S. Nakadata, J. Crystal Growth 129 (1992) 706.

[15] M. Mantani, M. Sugiyama, T. Ogawa, J. Crystal Growth 114 (1991) 71.

[16] D. C. Yin, Y. Inatomi, K. Kuribayashi, J. Crystal Growth 226 (2001) 534.

[17] L. Duan, J. Z. Shu, J. Crystal Growth 223 (2001) 181.

[18] W. B. Hou, A. B. Kudryavtsev, T. L. Bray, L. J. DeLucas, W. W. Wilson, J. Crystal Growth 232 (2001) 265.

[19] S. Miyashita, S. Komatsu, Y. Suzuki, T. Nakada, J. Crystal Growth 141 (1994) 419.

[20] H. Komatsu, S. Miyashita, Y. Suzuki, Jpn. J. Appl. Phys. 32 (1993) 1855.

[21] J. M. Garcia-Ruiz, M. L. Novella, F. Otalora 196, (1999) 703.

[22] A. McPherson, A. J. Malkin, Y. G. Kutsunetsov, S. Koszelak, A. Wells, G. Jenkins, J. Howard, G. Lawson, J. Crystal Growth 196 (1999) 572.

[23] J. M. Mehta, Appl. Opt. 29 (1990) 1924.

[24] P. J. Shlichta, J. Crystal Growth 76 (1986) 656.

[25] A. A. Chernov, L. N. Rashkovich, A. A. Mkrtchan, J. Crystal Growth 74 (1986) 101.

[26] A. A. Chernov, L. N. Rashkovich, J. Crystal Growth 84 (1987) 389.

[27] P. G. Vekilov, L. A. Monaco, F. J. Rosenberger, J. Crystal Growth 148 (1995) 289.

[28] N. J. Booth, B. Stanojev, A. A. Chernov, P. G. Vekilov, Rev. Sci. Instruments, 73 (2002) 3540.

[29] J. H. Bruning, D. R. Herriott, J. E. Gallagher, D. P. Rosenfeld, A. D. White, D. J. Brangaccio, Appl. Opt. 13 (1974) 2693.

[30] B. V. Dorrio J. L. Fernandez, Meas. Sci. Technol., 10 (1999) R33.

[31] Y. Inatomi, H. Miyashita, E. Sato, K. Kuribayashi, K. Itonaga, T. Motegi, J. Cryst. Growth 30 (1993) 85.

[32] W. J. Fredericks, M. C. Hammonds, S. B. Howard, F. Rosenberger, J. Crystal Growth 141 (1994) 183.

[33] F. Otalora, M. L. Novella, D. Rondon, J. M. Garcia-Ruiz, J. Crystal Growth 196 (1999) 649.

[34] V. Ball, J. J. Ramsden, Biopolymers 46 (1998) 489.

[35] H. Lin, F. Rosenberger, J. Alexander, A. Nadarajah, J. Crystal Growth 151 (1995) 153.

[36] A. V. Elgersma, M. Ataka, T. Katsura, J. Crystal Growth 122 (1992) 31.

[37] D. C. Yin, Y. Inatomi, N. I. Wakayama, W. D. Huang, Acta Cryst. D., 2003, (in press)

Figure captions:

Fig. 1. Front (a) and upper (b) views of the cell used in this study. The laser light beam is normal to the front side of the cell. The dashed line in (a) is the reference line for the elimination of the environmental error.

Fig. 2. Concentration measurement system. (a) Schematic illustration of the measurement system: a Mach-Zehnder interferometer and the image processing system; (b) the sample cell and sample holder which are installed in the Mach-Zehnder interferometer. LD: laser diode, the light source; BS1~BS2: beam splitters; M1~M2: mirrors; W: fringe adjusting wedges; CP: compensator; VCR: video cassette recorder; L: the light beam direction.

Fig. 3. A block diagram of the measurement programs. It consists of two parts: a main program for the spatial concentration acquisition and a display program to show the time dependence of the concentration in real time.

Fig. 4. Schematically illustration of the temperature program for the dissolution experiment. The bold dashed line (a) and bold solid line (b) are the temperature programs at the upper side and the lower side of the cell, respectively.

Fig. 5. Example of the procedures of the concentration measurement: (a) an interferogram captured 30 min after the start of the dissolution; (b) interference intensity distribution of one scanning line at 3mm above from the cell bottom; (c) phase map (unwrapped) at 30min after the start of the dissolution; (d) concentration map at 30min after the start of the dissolution.

Fig. 6. Example of the time course of the variations: (a) time course evolution of the phase at two points; (b) time course evolution of the concentration at two points. In the figures, 2mm and 3mm represent the variations of the points at 2 and 3mm above the cell bottom, respectively. Both points are at the center of the horizontal line.

Fig. 7. Reproducibility of the lysozyme crystal growth processes under the same conditions but with different temperature control programs: comparison of the measured concentrations under temperature gradient control and isothermal conditions. The dashed lines and solid lines are the experimental runs under temperature gradient control (upper end of cell at 30°C, lower end of the cell at 10°C) and isothermal (at 20°C) conditions, respectively. Solution conditions in all experimental runs are the same. The concentration measurement started from the as-prepared solutions.

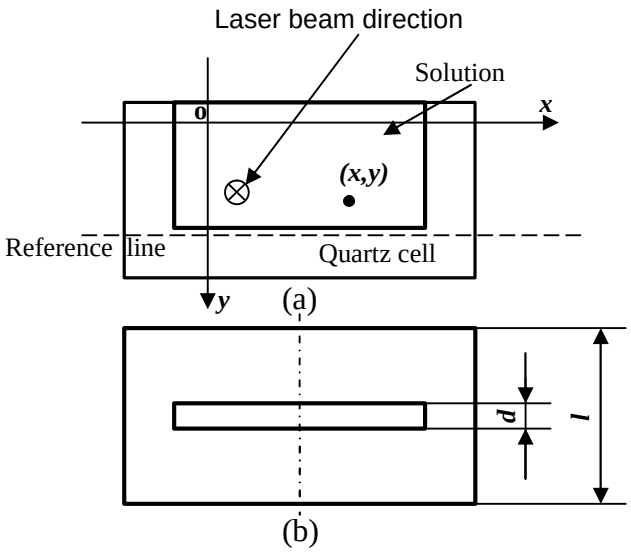
Laser beam direction
Solution
0
x
(x,y)
Reference line
Quartz cell
y
(a)
d
l
(b)

Fig.1.

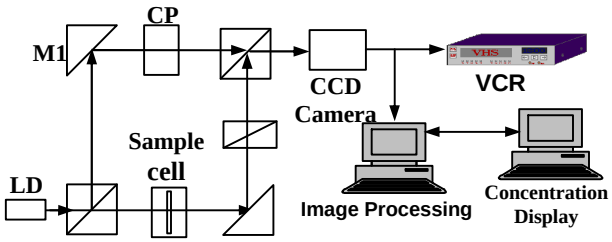
CP
M1
CCD
Camera
VCR
Sample
cell
LD
Image Processing
Concentration
Display

(a)

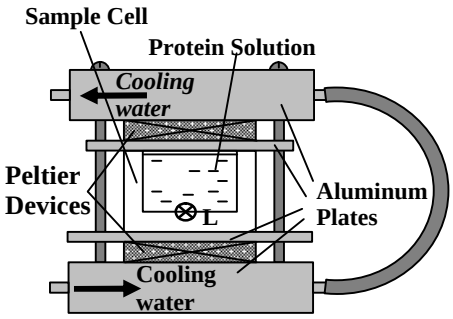
Sample Cell
Protein Solution
Cooling
water
Peltier
Devices
L
Aluminum
Plates
Cooling
water

(b)

Fig. 2.

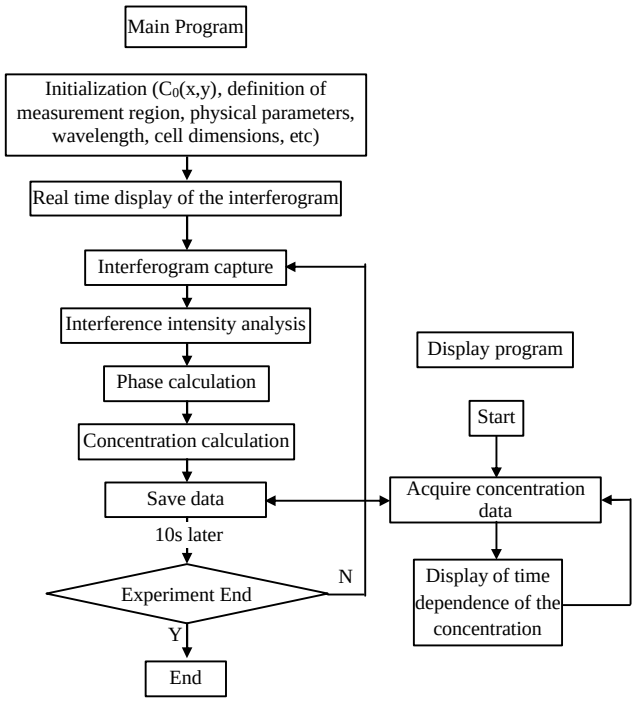
Main Program
Initialization (C_0(x,y), definition of measurement region, physical parameters, wavelength, cell dimensions, etc)
Real time display of the interferogram
Interferogram capture
Interference intensity analysis
Phase calculation
Concentration calculation
Save data
10s later
Experiment End
N
Y
End
Display program
Start
Acquire concentration data
Display of time dependence of the concentration

Fig. 3.

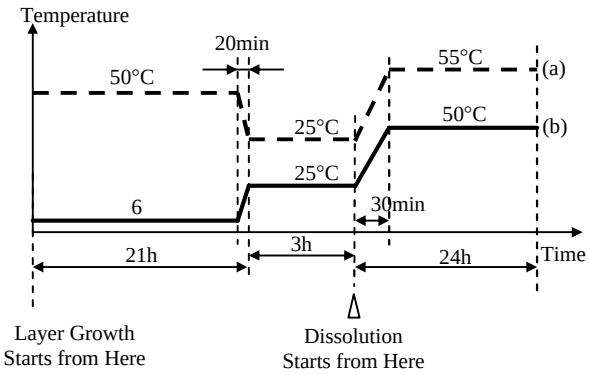
Temperature
20min
50°C
55°C
(a)
25°C
50°C
(b)
25°C
6
30min
21h
3h
24h
Time
Layer Growth
Starts from Here
Dissolution
Starts from Here

Fig. 4.

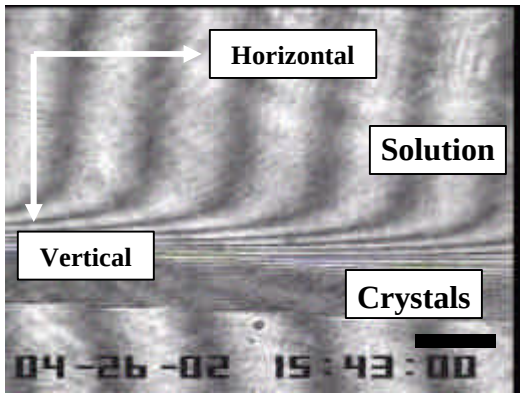
Horizontal
Solution
Vertical
Crystals
04-26-02 15:43:00

(a)

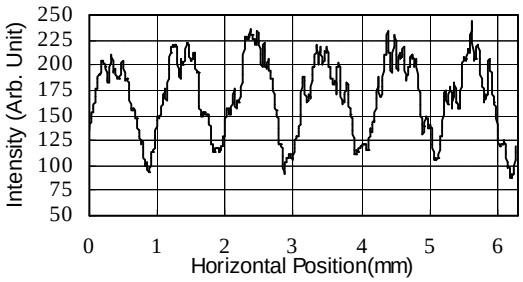
Intensity (Arb. Unit)
250
225
200
175
150
125
100
75
50
0 1 2 3 4 5 6
Horizontal Position(mm)

(b)

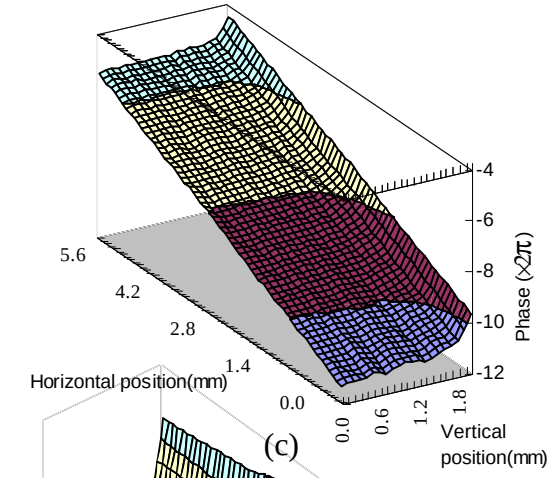
Phase (×2π)
-4
-6
-8
-10
-12
5.6
4.2
2.8
1.4
0.0
Horizontal position(mm)
0.0 0.6 1.2 1.8
Vertical position(mm)

(c)

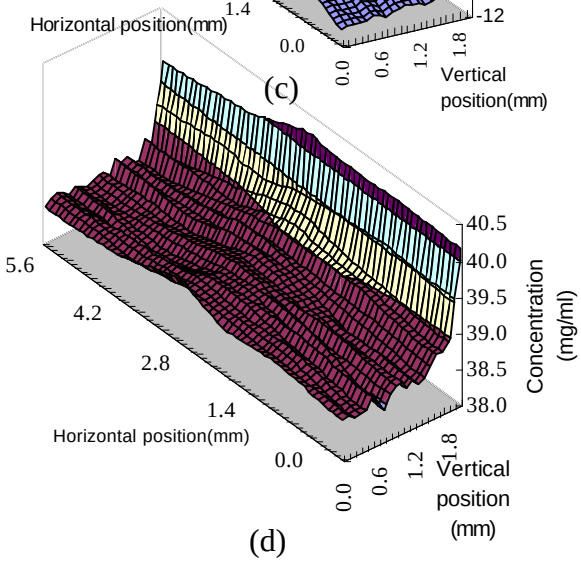
Concentration (mg/ml)
40.5
40.0
39.5
39.0
38.5
38.0
5.6
4.2
2.8
1.4
0.0
Horizontal position(mm)
0.0 0.6 1.2 1.8
Vertical position (mm)

(d)

Fig. 5.

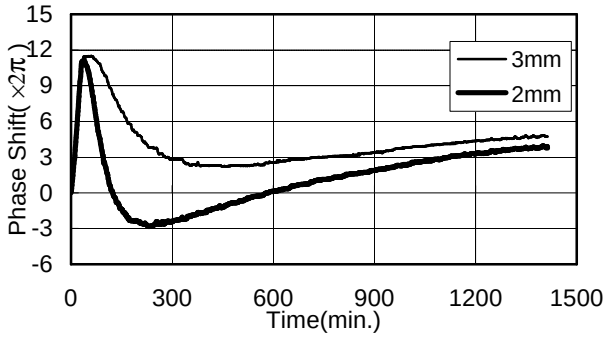
15
12
9
6
3
0
-3
-6
Phase Shift(×2π)
0
300
600
900
1200
1500
Time(min.)
3mm
2mm

(a)

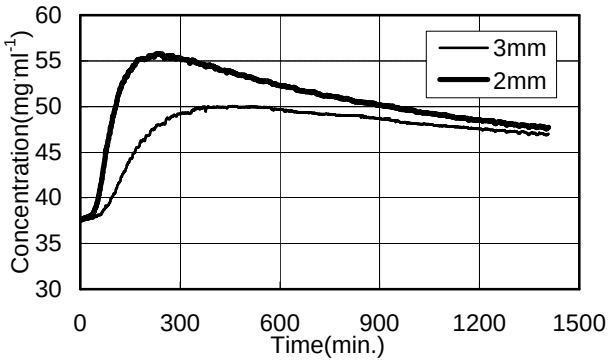
60
55
50
45
40
35
30
Concentration(mg·ml-1)
0
300
600
900
1200
1500
Time(min.)
3mm
2mm

(b)

Fig. 6.

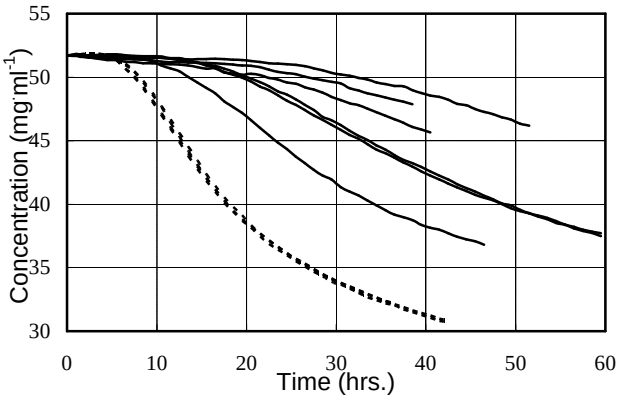
55
50
45
40
35
30
Concentration (mg·ml-1)
0
10
20
30
40
50
60
Time (hrs.)

Fig. 7.